ORGANOMETALLICS

Article

pubs.acs.org/Organometallics

Efficient Hydrogenation of Ketones and Aldehydes Catalyzed by Well-Defined Iron(II) PNP Pincer Complexes: Evidence for an Insertion Mechanism

Nikolaus Gorgas,[†] Berthold Stöger,[‡] Luis F. Veiros,[§] Ernst Pittenauer,[‡] Günter Allmaier,[‡] and Karl Kirchner*[,†]

[†]Institute of Applied Synthetic Chemistry and [‡]Institute of Chemical Technologies and Analytics, Vienna University of Technology, Getreidemarkt 9, A-1060 Vienna, Austria

[§]Centro de Química Estrutural, Instituto Superior Técnico, Universidade de Lisboa, Avenida Rovisco Pais No. 1, 1049-001 Lisboa, Portugal

Supporting Information

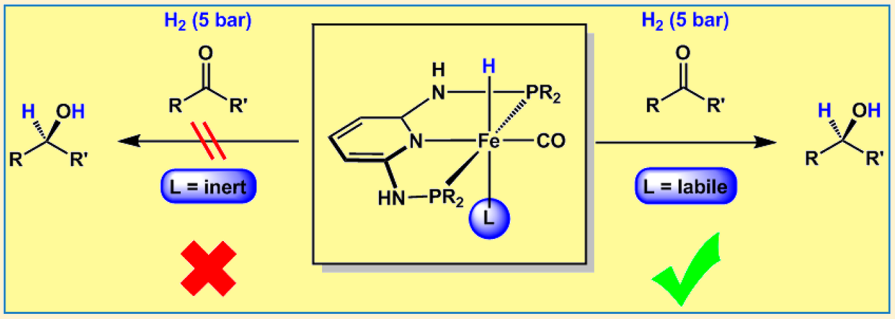

ABSTRACT: We have prepared and structurally characterized a new class of Fe(II) PNP pincer hydride complexes [Fe(PNP-*i*Pr)(H)(CO)(L)]^n (L = Br^-, CH_3CN, pyridine, PMe_3, SCN^-, CO, BH_4^-; n = 0, +1) based on the 2,6-diaminopyridine scaffold where the $PiPr_2$ moieties of the PNP ligand are connected to the pyridine ring via NH and/or NMe spacers. Complexes [Fe(PNP-*i*Pr)(H)(CO)(L)]^n with labile ligands (L = Br^-, CH_3CN, BH_4^-) and NH spacers are efficient catalysts for the hydrogenation of both ketones and aldehydes to alcohols under mild conditions, while those containing inert ligands (L = pyridine, PMe_3, SCN^-, CO) are catalytically inactive. Interestingly, complex [Fe(PNP^{Me}-*i*Pr)(H)(CO)(Br)], featuring NMe spacers, is an efficient catalyst for the chemoselective hydrogenation of aldehydes. The first type of complexes involves deprotonation of the PNP ligand as well as heterolytic dihydrogen cleavage via metal-alkoxide cooperation, but no reversible aromatization/deprotonation of the PNP ligand. In the case of the N-methylated complex the mechanism remains unclear, but obviously does not allow bifunctional activation of dihydrogen. The experimental results complemented by DFT calculations strongly support an insertion of the C═O bond of the carbonyl compound into the Fe−H bond.

INTRODUCTION

The catalytic reduction of polar multiple bonds via molecular hydrogen plays a significant role in modern synthetic organic chemistry. This reaction is excellently performed by many transition metal complexes containing noble metals such as ruthenium, rhodium, or iridium.[1] However, the limited availability of precious metals, their high price, and their toxicity diminish their attractiveness in the long run, and more economical and environmentally friendly alternatives have to be found. In this respect, the preparation of well-defined iron-based catalysts of comparable activity would be desirable.[2] Iron is the most abundant transition metal in the earth's crust and is ubiquitously available. Accordingly, it is not surprising that the field of iron-catalyzed hydrogenations of polar multiple bonds is rapidly evolving, as shown by several recent examples.[3−7]

It is interesting to note that many of these hydrogenations involve ligand−metal bifunctional catalysis (metal−ligand cooperation);[8] that is, the complexes contain electronically coupled hydride and acidic hydrogen atoms as a result of heterolytic dihydrogen cleavage that may be transferred to polar unsaturated substrates in an outer-sphere fashion or may be transferred via hydride migration (inner-sphere mechanism). An effective way of bond activation by metal−ligand cooperation involves aromatization/dearomatization of the ligand in pincer-type complexes. In particular, pincer ligands in which a central pyridine-based backbone is connected with $-CH_2PR_2$ and/or $-CH_2NR_2$ substituents were shown to exhibit this behavior.[9] This has resulted in the development of novel and unprecedented iron catalysis where this type of cooperation plays a key role in the heterolytic cleavage of H_2.[4] In the case of ketones and aldehydes, most efficient are

Received: September 26, 2014
Published: November 17, 2014

   dx.doi.org/10.1021/om5009814 | *Organometallics* 2014, 33, 6905−6914

complexes of the types [Fe(PNP^{CH2}-*i*Pr)(CO)(H)(Br)] and [Fe(PNP^{CH2}-*i*Pr)(CO)(H)(κ^1-BH_4)], where the bromide and BH_4^- ligands are labile, facilitating the coordination of the substrates. It has thus been suggested by Milstein that this reaction proceeds via an inner-sphere mechanism involving insertion of the carbonyl compounds into the Fe−H bond.[4a,c]

We are currently focusing on the synthesis and reactivity of iron complexes containing PNP pincer ligands based on the 2,6-diaminopyridine scaffold. In these ligands the aromatic pyridine ring and the phosphine moieties are connected via NH, *N*-alkyl, or *N*-aryl linkers. The advantage of these ligands is that both substituents of the phosphine and amine sites can be systematically varied in a modular fashion, which has a decisive effect on the outcome of reactions.[10] Recently we prepared the cationic Fe(II) hydride complex *cis*-[Fe(PNP-*i*Pr)$(CO)_2$H]$^+$, which involved reversible NH activation as well as heterolytic dihydrogen cleavage via metal−PNP ligand cooperation.[11] This complex turned out to be catalytically inactive for the hydrogenation of ketones and aldehydes, which was attributed to the fact that this complex is substitutionally inert and/or that the basicity of the hydride is too low.

Herein we report the synthesis, characterization, and catalytic activity of a series of neutral iron hydride complexes of the type [Fe(PNP-*i*Pr)(CO)(H)(Br)] (**2a−c**) where the P*i*Pr$_2$ moieties of the PNP ligand are connected to the pyridine ring via NH and/or NMe spacers (Scheme 1). In addition, the synthesis of a series of neutral and cationic hydride complexes of the type [Fe(PNP-*i*Pr)(CO)(H)(L)]^n (**3a−g**) (n = +1, 0) where L = CH_3CN, pyridine, PMe_3, κ^1-N-coordinated SCN^-, and κ^1-coordinated BH_4^- is described. All complexes featuring labile ligands L (Br^-, CH_3CN, BH_4^-) are efficient catalysts for the hydrogenation of ketones and aldehydes to alcohols under mild conditions. Moreover, the *N*-methylated complex **2b** is a chemoselective catalyst for the reduction of aldehydes. The first example of catalytic hydrogenation of aldehyde that is chemoselective against ketone was recently reported by Beller.[12] However, this reaction required elevated temperatures (120 °C) and a high H_2 pressure (20 bar). The experimental results are complemented by DFT calculations.

Scheme 1. Two Types of Highly Reactive Iron PNP Pincer Hydrogenation Catalysts

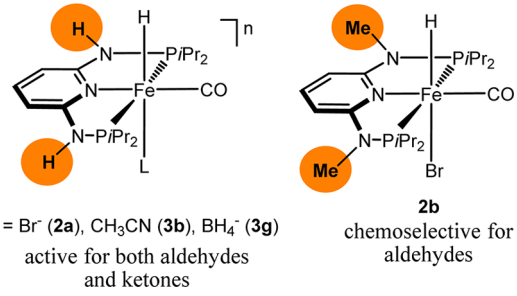

L = Br^- (**2a**), CH_3CN (**3b**), BH_4^- (**3g**)
active for both aldehydes and ketones

2b
chemoselective for aldehydes

RESULTS AND DISCUSSION

The synthesis of complexes [Fe(PNP-*i*Pr)(CO)(H)(Br)] (**2a−c**) was accomplished in 63−67% isolated yields by treatment of anhydrous $FeBr_2$ with 1 equiv of the corresponding PNP-*i*Pr ligands **1a−c** in THF in the presence of CO and subsequent addition of 1.1 equiv of Na[$HBEt_3$] (Scheme 2). This reaction proceeds via the intermediacy of the dibromo complexes [Fe(PNP-*i*Pr)$(CO)(Br)_2$], which, in principle, can be isolated in pure form as shown previously,[13] but are labile, slowly losing CO, and were thus directly used without prior isolation. In the case of the symmetrical *N*-methylated PNP-*i*Pr ligand **1b**, two isomers were obtained in a ca. 2.7:1 ratio with the hydride ligand being *trans* to the bromide and to the CO ligand, respectively, which could not be separated. All hydride complexes are air sensitive both in the solid state and in solution.

Characterization was accomplished by elemental analysis and by ^{1}H, ^{13}C{^{1}H}, and ^{31}P{^{1}H} NMR and IR spectroscopy. The ^{1}H NMR spectrum confirmed the presence of one hydride ligand, which appeared at −21.4, −21.6, and −21.8 ppm, respectively, as a well-resolved triplet with a $^2J_{HP}$ coupling constant of about 57 Hz. Isomer **2b′** exhibits the hydride resonance at −1.1 ppm. In the ^{13}C{^{1}H} NMR spectrum the most noticeable resonance is the low-field resonance of the carbonyl carbon atom *trans* to the pyridine nitrogen observed as a triplet in the range 217.1−222.7 ppm (J_{CP} about 13−23 Hz). The ^{31}P{^{1}H} NMR spectra of complexes **2a** and **2b** give rise to a singlet at 147.1 and 164.0 ppm, respectively, while in the case of **2c** two doublets centered at 165.0 and 147.2 ppm are observed. In the IR spectrum the strong bands for CO stretching frequencies are found in the range 1901 to 1903 cm^{-1}.

The solid-state structure of **2a** was determined by single-crystal X-ray diffraction. A structural view is depicted in Figure 1 with selected bond distances given in the caption. Complex **2a** adopts a distorted octahedral geometry around the metal center with the hydride ligand being in *cis* position to a CO ligand. The PNP ligand is coordinated to the iron center in a typical tridentate meridional mode, with a P1−Fe1−P2 angle of 164.58(4)°. The hydride and the N−H atoms could be unambiguously located in the difference Fourier maps. The Fe−H distance was refined to 1.46(2) Å.

Complexes **2a−c** are substitutionally labile. This has been exemplarily studied in more detail with **2a** (Scheme 3). Dissolution of **2a** in MeOH-d_4 resulted in an immediate replacement of the Br^- ligand to give the cationic complex [Fe(PNP-*i*Pr)(H)(CO)(MeOH-d_4)]$^+$ (**3a**), as evident by a new hydride resonance at −26.6 ppm and a ^{31}P{^{1}H} signal at 140.6 ppm. Interestingly, in ethanol dissociation of the bromide

Scheme 2. Synthesis of Hydride Complexes 2a−c

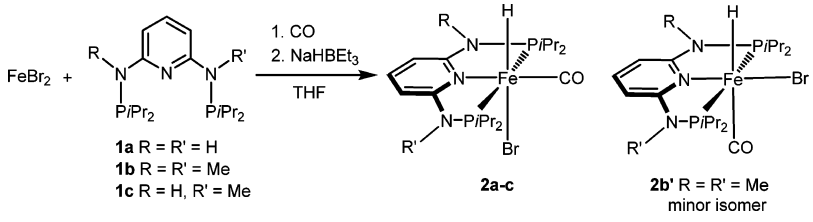

1a R = R′ = H
1b R = R′ = Me
1c R = H, R′ = Me

2a-c

2b′ R = R′ = Me
minor isomer

dx.doi.org/10.1021/om5009814 | *Organometallics* 2014, 33, 6905−6914

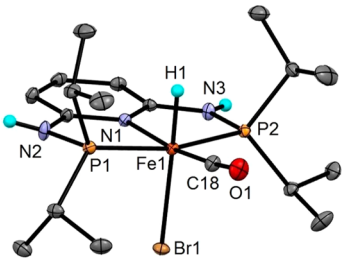

Figure 1. Structural view of [Fe(PNP-*i*Pr)(H)(CO)(Br)]·CH_2Cl_2 (**2a**·CH_2Cl_2) showing 50% thermal ellipsoids (CH_2Cl_2 and most hydrogen atoms omitted for clarity). Selected bond lengths (Å) and angles (deg): Fe1−P1 2.1927(6), Fe1−P2 2.1927(6), Fe1−N1 2.022(1), Fe1−Br1 2.5269(6), Fe1−C18 1.731(1), Fe1−H1 1.46(2), P1−Fe1−P2 164.58(1), N1−Fe1−C18 171.95(4).

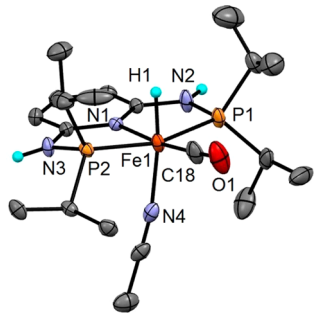

Figure 2. Structural view of [Fe(PNP-*i*Pr)(H)(CO)(CH_3CN)]Br (**3b**) showing 50% thermal ellipsoids (bromide counterion and most hydrogen atoms omitted for clarity). Only one of the two crystallographically independent complexes is shown. Selected bond lengths (Å) and angles (deg): Fe1−P1 2.1986(10), Fe1−P2 2.2028(10), Fe1−N1 1.998(2), Fe1−N4 1.984(2), Fe1−C18 1.738(3), Fe1−H1 1.460(6), P1−Fe1−P2 162.87(3), N1−Fe1−C18 173.7(1).

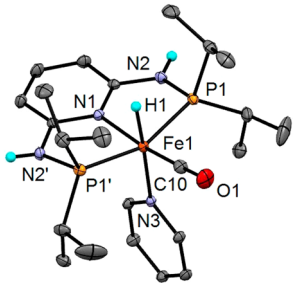

Figure 3. Structural view of [Fe(PNP-*i*Pr)(H)(CO)(py)]BF_4 (**3c**) showing 50% thermal ellipsoids (most hydrogen atoms and BF_4^- anion omitted for clarity). Selected bond lengths (Å) and angles (deg): Fe1−P1 2.1915(3), Fe1−N1 2.017(1), Fe1−N3 2.068(1), Fe1−C10 1.738(2), Fe1−H1 1.46(2), P1−Fe1−P2 158.56(1), N1−Fe1−C10 171.31 (6).

ligand is much less pronounced and Br^- is only partially replaced by EtOH. This might also contribute to the fact that higher catalytic activities are achieved in this solvent perhaps due to diminished competition between substrate and solvent for a free coordination site (*vide infra*). The addition of L = CH_3CN, pyridine, PMe_3, SCN^-, CO, and BH_4^- leads to the formation of the corresponding cationic or neutral complexes $[Fe(PNP\text{-}iPr)(H)(CO)(L)]^n$ (**3b−g**) as shown in Scheme 3. Complexes **3b−g** could also be isolated in pure form by reacting **2a** with the respective ligands CH_3CN (neat), pyridine, PMe_3 SCN^- (Na^+ salt), BH_4^- (Na^+ salt), and CO in both the absence and presence of silver salts in 83−97% isolated yields. These complexes exhibit the characteristic hydride resonances at −18.6, −20.1, −11.1, −19.8, −7.5, and −18.2, ppm, respectively. In the case of **3g** the BH_4^- ligand gives rise to a broad signal at −3.61 ppm (4H). The observation of a broad four-proton resonance in this region of the ^1H NMR spectrum is typical for κ^1-coordinated BH_4^- ligands of iron complexes and indicates dynamic behavior of this ligand.[4c]

Structural views of **3b**, **3c**, **3d**, **3e**, and **3g** are depicted in Figures 2−6 with selected bond distances given in the captions.

The lability of complexes **2a** and **3b−g** was also studied by ESI-MS. Solutions of these complexes in CH_3CN were subjected to ESI-MS analysis in the positive ion mode (the neutral complexes were investigated in the presence of NaCl to obtain cationic sodiated species). In the case of [Fe(PNP-*i*Pr)(H)(CO)(Br)] (**2a**), $[Fe(PNP\text{-}iPr)(H)(CO)(CH_3CN)]^+$ (**3b**), and [Fe(PNP-*i*Pr)(H)(CO)(κ^1-BH_4)] (**3g**) the cationic fragment $[Fe(PNP\text{-}iPr)(H)(CO)]^+$ (*m*/*z* 426.1) was found as the predominant species, while for all other complexes $[Fe(PNP\text{-}iPr)(H)(CO)(py)]^+$ (**3c**), $[Fe(PNP\text{-}iPr)(H)(CO)(PMe_3)]^+$ (**3d**), [Fe(PNP-*i*Pr)(H)(CO)(κ^1-*N*-SCN)] (**3e**), and $[Fe(PNP\text{-}iPr)(H)(CO)_2]^+$ (**3f**) the intact complexes $[M]^+$ (*m*/*z* 505.1, 502.2, 507.1 (as $[M + Na]^+$, and 456.1) were observed as major fragments. We also investigated an EtOH solution of **2a** in the presence of KO*t*Bu in the hopes of detecting the alkoxide complex [Fe(PNP-*i*Pr)(H)(CO)(OEt)]. However, only the fragment at *m*/*z* 426.1 was detected as the major species. These observations are in accord with the fact that the ligands Br^-, OEt^-, BH_4^-, and CH_3CN *trans* to the hydride ligand are substitutionally labile, while pyridine, PMe_3, SCN^-, and CO are substitutionally inert.

The catalytic activity of all hydride complexes was investigated in the hydrogenation of ketones and aldehydes. In preliminary experiments various solvents were tested for the

Scheme 3. Substitution of the Bromide Ligand in 2a by MeOH-d_4, CH_3CN, Pyridine, PMe_3, SCN^-, CO, and BH_4^-

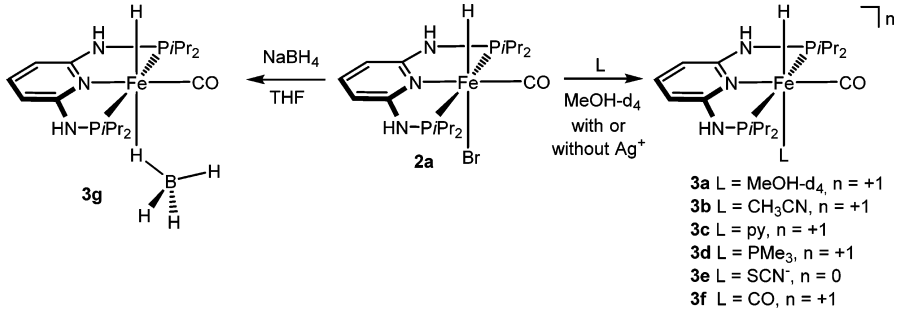

dx.doi.org/10.1021/om5009814 | *Organometallics* 2014, 33, 6905−6914

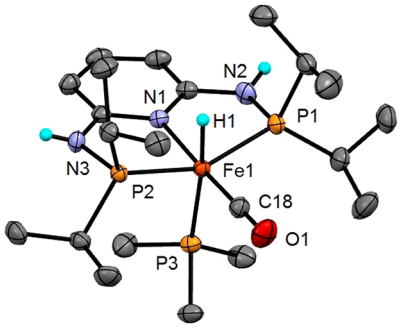

Figure 4. Structural view of [Fe(PNP-*i*Pr)(H)(CO)(PMe_3)]BF_4 (**3d**) showing 50% thermal ellipsoids (most hydrogen atoms and BF_4^- anion omitted for clarity). Selected bond lengths (Å) and angles (deg): Fe1−P1 2.1952(4), Fe1−P2 2.1886(4), Fe1−N1 2.007(1), Fe1−C18 1.730(2), Fe1−P3 2.2753(5), Fe1−H1 1.46(2), P1−Fe1−P2 154.89(2), N1−Fe1−C18 176.68(7).

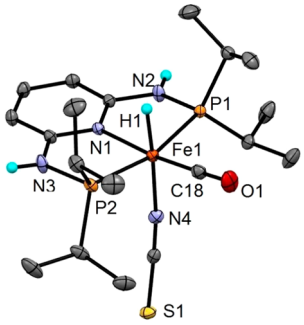

Figure 5. Structural view of [Fe(PNP-*i*Pr)(H)(CO)(κ^1-*N*-SCN)] (**3e**) showing 50% thermal ellipsoids (most hydrogen atoms omitted for clarity). Selected bond lengths (Å) and angles (deg): Fe1−P1 2.1884(7), Fe1−P2 2.1871(7), Fe1−N1 2.018(1), Fe1−N4 1.989(1), Fe1−C18 1.738(2), Fe1−H1 1.49(2), P1−Fe1−P2 164.78(1), N1−Fe1−C18 172.84(5).

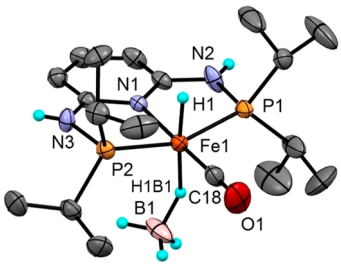

Figure 6. Structural view of [Fe(PNP-*i*Pr)(H)(CO)(κ^1-BH_4)] (**3g**) showing 50% thermal ellipsoids (most hydrogen atoms omitted for clarity). Selected bond lengths (Å) and angles (deg): Fe1−P1 2.1885(7), Fe1−P2 2.1873(7), Fe1−N1 1.998(2), Fe1−C18 1.733(2), Fe1−B1 2.72(1), Fe1−H1 1.46(2), Fe1−H1B1 1.67(2), P1−Fe1−P2 159.99(3), N1−Fe1−C18 178.13(9).

hydrogenation of acetophenone using 1.0 mol % **2a**, 2.0 mol % KO*t*Bu, and 5 bar hydrogen at ambient temperature (25 °C, Table 1). The hydrogenation reaction takes place only in alcoholic solutions, with ethanol being by far the best solvent, giving *rac*-1-phenylethanol in essentially quantitative yield. Moreover, in the absence of base and/or H_2 no reaction takes place, indicating that **2a** is not an active catalyst for transfer hydrogenation. The amount of the catalyst precursor could be reduced to 0.1 mol %. In this case 77% isolated yield was reached within 1 h, which corresponds to a TOF of 770 h^{-1}.

Table 1. Iron-Catalyzed Hydrogenation of Acetophenone[a]

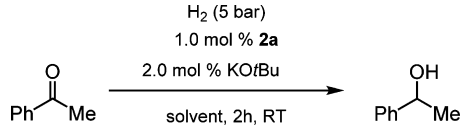

entry	solvent	yield [%][b]	TOF [h^{-1}]
1	THF		
2	MeOH	36	18
3	*i*PrOH	58	29
4	*t*AmylOH	89	45
5	EtOH	99	50

[a]Reaction conditions: **2a** (0.025 mmol, 1.0 mol %), KO*t*Bu (0.05 mmol), substrate (2.5 mmol), solvent (5 mL), H_2 (5 bar), 2 h. [b]Yields were determined by ^{1}H NMR.

However, in terms of a better reproducibility 0.5 mol % catalyst was used for all subsequent reactions.

In contrast to **2a**, under the same reaction conditions, as well as with even 5 mol %, complex **2b**, bearing NMe linkers, was completely inactive for the reduction of ketones, while **2c**, containing one NH and one NMe linker, was catalytically active but with a significantly lower activity than **2a** (28% yield). On the other hand, the catalytic activity of both [Fe(PNP-*i*Pr)(H)(CO)(CH_3CN)]$^+$ (**3b**) and Fe(PNP-*i*Pr)(H)(CO)-(κ^1-BH_4)] (**3g**) was similar to that of **2a** (94% yield). The reaction with **3g** could be performed even without addition of an external base, although slightly higher temperatures were required to achieve comparable activities (50 °C) since base has to be generated by alcoholysis of free BH_4^-.[14] Similar observations were recently made by Milstein.[4c] In sharp contrast to the substitutionally labile complexes **2a**, **3b**, and **3g**, the inert compounds **3c−f** were catalytically inactive.

On the basis of these results, we investigated the scope and limitations of catalyst **2a** using various substrates (Table 2). Halogen substituents had no notable influence on the catalytic activity, while the reaction with 4-methoxyacetophenone and 4-nitroacetophenone resulted in significantly lower yields (entries 5 and 6). Likewise, for simple ketones such as cyclohexanone and benzophenone lower activity was observed. In the presence of a nitrile or primary amine substituents on the aromatic system no reaction was observed, presumably due to preferential coordination of these groups to the iron center, thus blocking a vacant coordination site to accommodate an incoming substrate (entries 7 and 8). The same result was found for 4-acetylpyridine. This is in line with the observation that **3c**, containing a strongly bound pyridine ligand, is catalytically inactive. The reduction of 2-acetylpyridine was extremely efficient, giving full conversion even after 1 h (TOF = 200 h^{-1}, entry 11). In this case, coordination of pyridine is obviously hampered due to the bulky acetyl substituent in the *ortho* position of the pyridine unit. The reduction of *trans*-4-phenylbutenone resulted in mixtures, where reduction of the double bond also took place (entry 13). Finally, the hydrogenation of aldehydes was tested with complexes **2a** and **2b** as catalysts utilizing benzaldehyde, 4-isopropylbenzaldehyde, cyclohexane carboxaldehyde, picolinealdehyde, and isonicotinealdehyde (Table 3). Under the standard reaction conditions, low conversions were observed (entry 1). However, an increase of the catalyst loading to 5.0 mol % and reduction of the reaction time to 10 min afforded the respective alcohols in nearly quantitative yield. In the case of isonicotinealdehyde

dx.doi.org/10.1021/om5009814 | *Organometallics* 2014, 33, 6905−6914

Table 2. Iron-Catalyzed Hydrogenation of Ketones[a]

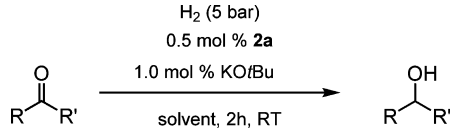

Entry	Substrate	Product	Yield[d] [%]	TOF [h^{-1}]
1	R = H		99	100
2[b]	R = H		77	770
3	R = Cl		99	100
4	R = Br		99	100
5	R = OMe		34	34
6	R = NO_2		47	47
7	R = NH_2			
8	R = CN			
9			30	30
10			64	64
11[c]			99	200
12				-
13			10	100
			45	
			45	

[a]Reaction conditions: **2a** (0.0125 mmol), KO*t*Bu (0.025 mmol), substrate (2.5 mmol), EtOH (5 mL), H_2 (5 bar), 2 h. [b]Reaction conditions: **2a** (0.0025 mmol), KO*t*Bu (0.005), substrate (2.5 mmol), EtOH (3 mL), 1 h. [c]Reaction time: 1 h. [d]Yields were determined by ^{1}H NMR.

Table 3. Iron-Catalyzed Hydrogenation of Aldehydes[a]

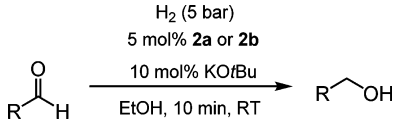

Entry	Substrate	Product	Yield[d] [%]	TOF [h^{-1}]
1[b]			23	23
2			99	120
3	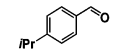	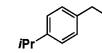	99	120
4[c]			99	60
5			99	120
6				

[a]Reaction conditions: **2a** or **2b** (0.125 mmol), KO*t*Bu (0.25 mmol), substrate (2.5 mmol), EtOH (5 mL), H_2 (5 bar), 10 min. [b]Reaction conditions: **2a** (0.0125 mmol), KO*t*Bu (0.025 mmol), substrate (2.5 mmol), EtOH (5 mL), H_2 (5 bar), 2 h. [c]Reaction time: 20 min. [d]Yields were determined by ^{1}H NMR.

Scheme 4. Dehydrohalogenation of 2a with KO*t*Bu in THF to Give A and Subsequent Addition of H_2 to Afford a Mixture of the *trans* and *cis* Dihydride Complexes 4a and 4b

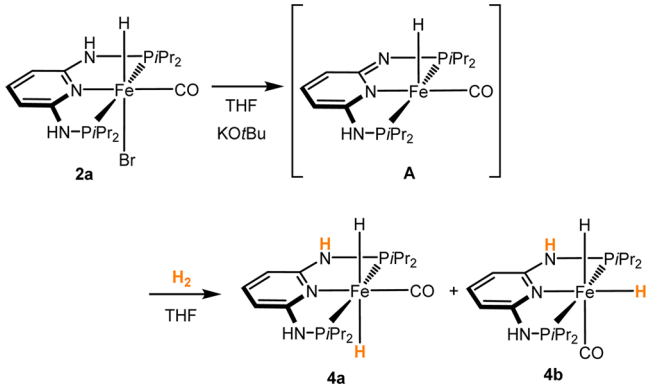

(entry 6) no reaction took place, again due to strong coordination of the pyridine moiety.

In order to gain a mechanistic understanding of the catalytic hydrogenation of aldehydes and ketones, some stoichiometric reactions of **2a** were investigated. Treatment of **2a** in THF with KO*t*Bu resulted in an immediate color change from orange to deep red. In the ^{1}H NMR spectrum hydride signals were no longer present, but in the IR spectrum two strong absorptions at 1872 and 1822 cm^{-1} were observed (ν_{Fe-H} and ν_{CO}). This may be tentatively assigned to the formation of [Fe(PNP^{-H}-*i*Pr)(H)(CO)] (**A**) as a result of dehydrohalogenation. In this context it is important to note that a series of related iron PNP pincer complexes were prepared and even structurally characterized recently by Schneider[15] and Jones.[16] The formation the Fe(0) dicarbonyl complex [Fe(PNP-*i*Pr)(CO)$_2$] can be ruled out by comparison with an authentic sample.[11] Moreover, purging the solution with H_2 afforded a mixture of the *trans* and *cis* dihydride complexes [Fe(PNP-*i*Pr)(CO)(H)$_2$] (**4a,b**) (Scheme 4). Such a reaction does not take place with [Fe(PNP-*i*Pr)(CO)$_2$]. The ^{1}H NMR spectrum of the mixture at room temperature exhibited a triplet at −9.02 ppm for the *trans*-dihydride **4a** and only one broad signal at −13.4 ppm for the *cis*-dihydride **4b** due to fast exchange between the two hydrides. Complexes **4a** and **4b** did not show any significant reactivity toward acetophenone even after 1 day, suggesting that these are not active species in the catalytic reduction of ketones. Our findings are fully consistent with Milstein's discoveries based on the related iron pincer complex (Fe-[PNP^{CH2}-*i*Pr)(H)(CO)(κ^1-BH$_4$)],[4c] but strongly contrast the recently reported computational study by Yang on the iron-catalyzed reduction of acetophenone.[17] In his calculated mechanism, the reaction proceeds via *trans*-[Fe(PNP-*i*Pr)-(CO)(H)$_2$] (**4a**) and involves an outer-sphere hydrogen transfer from this complex to the carbonyl carbon atom of acetophenone in EtOH as solvent. Accordingly, we believe that this mechanism is not operative in our system with respect to ketone reduction, although *trans*-dihydride iron PNP complexes were shown to be important species in other reactions.[4b,d,e,13,15,16,18] The reduction of aldehydes, in

dx.doi.org/10.1021/om5009814 | *Organometallics* 2014, 33, 6905−6914

particular with **2b**, remains mechanistically unclear at this stage, and the involvement of dihydride complexes cannot be ruled out.

In sharp contrast to the above observations in THF, when KO*t*Bu was added to an EtOH solution of **2a** in the presence of dihydrogen, no changes in the IR, ^{1}H NMR, and ^{31}P{^{1}H} NMR spectra were observed. This again emphasizes the particular role of EtOH as solvent apparently preventing the formation of **4a** and **4b**.

Preliminary DFT calculations[19] were carried out to establish a reasonable mechanism using the hydrogenation of acetaldehyde with **2a** as model. A summary of these results with the most relevant points along the catalytic cycle is presented in Scheme 5. Loss of a labile bromide ligand and

Scheme 5. Catalytic Cycle Calculated for an *Inner-Sphere* Mechanism[a]

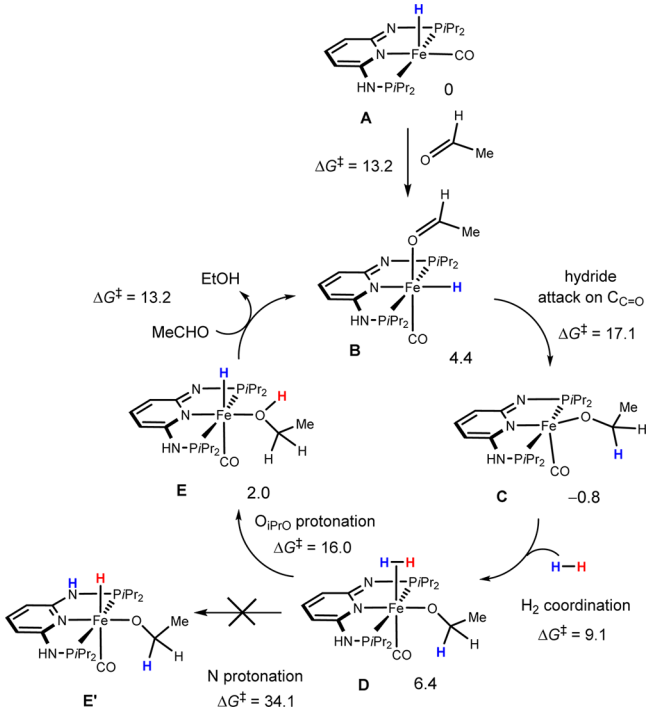

[a]Free energy values (in kcal/mol) referred to [Fe(PNP^{-H}-*i*Pr)(H)(CO)] (**A**).

deprotonation of an NH group in the catalytic precursor **2a** will produce a five-coordinated complex, [Fe(PNP^{-H}-*i*Pr)(H)(CO)] (**A**), that is the starting point in the mechanistic investigations and also the reference for all free energy values. The catalytic cycle depicted in Scheme 5 starts with the occupation of the free coordination site in **A** by the substrate (in **B**). Then there is nucleophilic attack of the hydride on the carbonyl C atom with formation of the alkoxide complex, **C**. The reaction proceeds with coordination of dihydrogen (**D**) and subsequent protonation of the O atom with formation of the alcohol and regeneration of the hydride (**E**). The cycle is closed by ligand exchange with liberation of one molecule of the product and coordination of another substrate from **E** back to **B**. The highest energy barrier along the cycle corresponds to the hydride migration step, and its value (17.1 kcal/mol) indicates a facile reaction. It has to be emphasized that the PNP ligand is not involved in dihydrogen activation but remains deprotonated throughout the catalytic cycle, acting as a strongly electron-donating anionic ligand. In fact, the activation barrier for dihydrogen splitting involving protonation of the PNP N atom, corresponding to reversible aromatization/dearomatization of that ligand to afford **E′**, is considerably higher (34.1 kcal/mol) than the one associated with protonation of the O atom of the alkoxide producing the final alcohol product as shown in Scheme 5 (16.0 kcal/mol).

The dihydrogen splitting step was also studied with the inclusion of one explicit solvent molecule (ethanol) in the calculations (Scheme 6). In fact, the ethanol molecule acting as

Scheme 6. Dihydrogen Splitting via O- and N-Protonation Calculated with One Explicit EtOH Molecule[a]

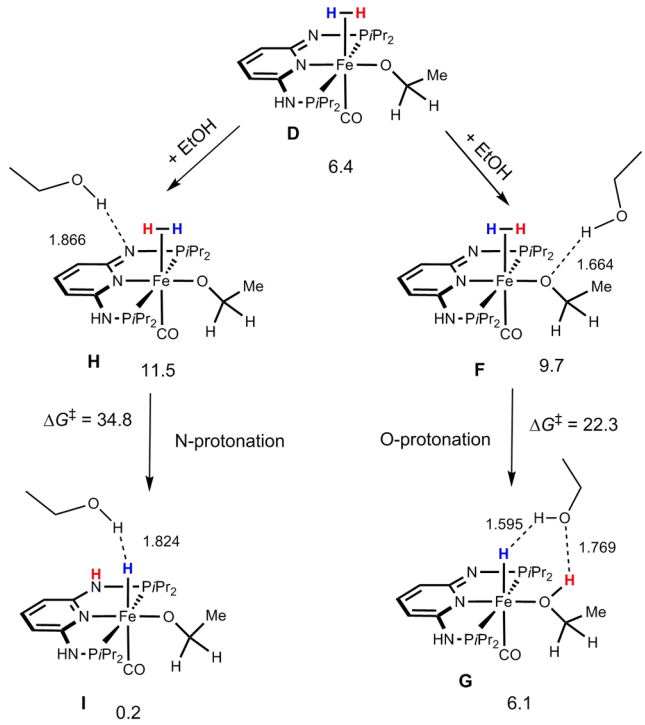

[a]Free energy values (in kcal/mol) are referred to [Fe(PNP^{-H}-*i*Pr)(H)(CO)] (**A**) and H-bond distances in Å.

a proton shuttle could alter the most favorable path and change the conclusions above. The results obtained are shown in Scheme 6 and indicate that O-protonation of the alkoxide ligand remains the preferred pathway for the reaction, with a barrier 12.5 kcal/mol lower than the value calculated for protonation of the PNP N atom. The O-protonation step calculated with an explicit solvent molecule (EtOH), represented in Scheme 6, has a free energy barrier 6.3 kcal/mol higher than the same process calculated without the ethanol molecule (cf. Scheme 5) due to the rise in the entropy term originated by the presence of that extra molecule. If one compares energy values, the barrier becomes 5 kcal/mol lower in the case with the extra ethanol molecule. This result confirms that the PNP ligand remains deprotonated and, thus, dearomatized along the entire cycle and means that N−H acidity has no active part in the reaction mechanism that should not be classified as bifunctional catalysis in this case.

It is also interesting to note that deprotonation of the PNP ligand is accompanied by a substantial increase of the ligand charge. In fact, in the N-protonated counterpart of **A**, [Fe(PNP-*i*Pr)(H)(CO)]$^{+}$, the PNP ligand is more positive (C_{PNP} = 1.03)

dx.doi.org/10.1021/om5009814 | *Organometallics* 2014, 33, 6905−6914

than the same ligand in **A** (C_{PNP} = 0.14). Accordingly, the hydride in the cationic complex is also electron poorer than the equivalent ligand in **A**, C_H = −0.14 and −0.16, respectively, indicating that **A** should be a better active species in a reaction where the key step is hydride nucleophilic attack on the substrate carbonyl C atom.

CONCLUSION

In conclusion, we have prepared a new class of Fe(II) PNP pincer hydride complexes [Fe(PNP-*i*Pr)(CO)(H)(L)]^n (**2a−c**, **3a−g**) (n = +1, 0) based on the 2,6-diaminiopyridine scaffold where the P*i*Pr$_2$ moieties of the PNP ligand connect to the pyridine ring via NH and/or NMe spacers and where the complexes feature both labile (Br^-, CH_3CN, BH_4^-) and inert (pyridine, PMe_3, SCN^-, CO) coligands. Complexes with labile ligands are efficient catalysts for the hydrogenation of ketones and aldehydes to alcohols under mild conditions. These reactions take place at room temperature with turnover frequencies up to 770 h^{-1} using 5 bar hydrogen pressure and seem to involve heterolytic dihydrogen cleavage via metal-alkoxide cooperation, with the PNP ligand not being involved in dihydrogen activation. The PNP ligand remains deprotonated throughout the catalytic cycle, acting as a strongly electron donating anionic ligand. The catalytic reactions do not proceed in aprotic solvents, but require alcoholic solutions, with EtOH being the best solvent. EtOH prevents the formation of dihydride species, which are catalytically inactive, and seems to stabilize the dearomatized 16*e* intermediate **A** due to reversible EtOH coordination. The experimental results complemented by DFT calculations strongly support an inner-sphere mechanism, i.e., insertion of the C═O bond of the carbonyl compound into the Fe−H bond. Finally, the chemoselectivity of **2b** toward aldehydes vs ketones is remarkable and may be synthetically useful. This reaction apparently also does not proceed via a bifunctional mechanism. Detailed mechanistic studies, in particular the reaction of catalyst **2b** where the mechanism remains unclear, as well as catalyst optimizations are currently under way.

EXPERIMENTAL SECTION

General Procedures. All manipulations were performed under an inert atmosphere of argon by using Schlenk techniques or in an MBraun inert-gas glovebox. The solvents were purified according to standard procedures.[20] The deuterated solvents were purchased from Aldrich and dried over 4 Å molecular sieves. The ligands *N*,*N*′-bis(diisopropylphosphino)-2,6-diaminopyridine (PNP-*i*Pr) (**1a**),[21] *N*,*N*′-bis(diisopropylphosphino)-*N*,*N*′-dimethyl-2,6-diaminopyridine (PNP^{Me}-*i*Pr) (**1b**), and *N*,*N*′-bis(diisopropylphosphino)-*N*-methyl-2,6-diaminopyridine (PNP^{H,Me}-*i*Pr) (**1c**)[22] and complex [Fe(PNP-*i*Pr)(H)(CO)$_2$]SbF$_6$ (**3f**) were prepared according to the literature.[11] ^{1}H, ^{13}C{^{1}H}, and ^{31}P{^{1}H} NMR spectra were recorded on Bruker AVANCE-250 and AVANCE-400 spectrometers. ^{1}H and ^{13}C{^{1}H} NMR spectra were referenced internally to residual protio-solvent and solvent resonances, respectively, and are reported relative to tetramethylsilane (δ = 0 ppm). ^{31}P{^{1}H} NMR spectra were referenced externally to H_3PO_4 (85%) (δ = 0 ppm). All mass spectrometric measurements were performed on an Esquire 3000^{plus} 3D-quadrupole ion trap mass spectrometer (Bruker Daltonics, Bremen, Germany) in positive-ion mode electrospray ionization (ESI-MS). All mass calculations are based on the lowest mass (i.e. most abundant) iron isotope (^{56}Fe-isotope).

General Procedure for the Hydrogenation Reactions. All hydrogenation reactions were performed at ambient temperature (25 °C) under a hydrogen atmosphere of 5 bar using a 90 mL Fisher-Porter tube, which was flushed several times with hydrogen gas prior to the addition of the reaction solution. For the preparation of the reaction solutions a vial was charged with the specified amount of catalyst, substrate, and EtOH. Subsequently, KO*t*Bu was added and the solution was taken up into a syringe and transferred to the Fisher-Porter tube. After stirring the solution for the stated time, pressure was carefully released, diethyl ether (20 mL) was added, and the reaction was quenched by addition of an aqueous solution of H_3PO_4 (0.5 M, 0.5 mL). The organic phase was separated, washed with brine, and dried over $MgSO_4$. The solvent was removed under reduced pressure, and the isolated product was characterized by NMR spectroscopy.

Syntheses. [Fe(PNP-*i*Pr)(H)(CO)Br] (2a). Anhydrous $FeBr_2$ (190 mg, 0.88 mmol) and **1a** (300 mg, 0.88 mmol) were dissolved in 12 mL of THF. The immediately formed yellow suspension was stirred for 1 h at room temperature before CO was bubbled through the reaction mixture for 10 min. During this time the color of the suspension changed from yellow to blue. The reaction mixture was cooled to 0 °C, and a solution of Na[HBEt$_3$] in toluene (0.97 mL, 1 M, 0.97 mmol) was slowly added. The reaction mixture was stirred for 30 min at 0 °C, in which time the color changed from blue to dark red. After an additional 60 min at room temperature the solution was filtered and the solvent was removed under reduced pressure. The dark residue was taken up in THF (3 mL), and the product was precipitated by addition of *n*-hexane (15 mL). The precipitate was separated from the supernatant solution, washed with *n*-pentane (3 × 10 mL), and dried under vacuum to afford a bright yellow powder. Yield: 298 mg (67%). Anal. Calcd for $C_{18}H_{34}BrFeN_3OP_2$: C, 42.71; H, 6.77; N, 8.30. Found: C, 42.57; H, 6.83; N, 8.33. ^{1}H NMR (δ, CD_2Cl_2, 20 °C): 7.17 (t, J = 8.0 Hz, 1H, py^4), 6.11 (d, J = 8.0 Hz, 2H, py^{3,5}), 5.54 (bs, 2H, N*H*), 3.24 (m, 2H, C*H*(CH$_3$)$_2$), 2.51 (m, 2H, C*H*(CH$_3$)$_2$), 1.56 (dd, J = 7.9 Hz, J = 17.6, 6H, CH(C*H*$_3$)$_2$), 1.44 (dd, J = 6.4 Hz, J = 11.9, 6H, CH(C*H*$_3$)$_2$), 1.21 (dd, J = 7.0 Hz, J = 17.1, 6H, CH(C*H*$_3$)$_2$), 1.00 (dd, J = 6.8 Hz, J = 14.2, 6H, CH(C*H*$_3$)$_2$), −21.36 (t, $^2J_{HP}$ = 56.6, 1H, Fe*H*). ^{13}C{^{1}H} NMR (δ, CD_2Cl_2, 20 °C): 222.7 (br, CO), 160.8 (t, $^2J_{CP}$ = 9.9 Hz, py^{2,6}), 138.7 (s, py^4), 97.4 (s, py^{3,5}), 30.3 (t, $^1J_{CP}$ = 10.7 Hz, CH(CH$_3$)$_2$), 27.4 (t, $^1J_{CP}$ = 12.9 Hz, CH(CH$_3$)$_2$), 19.6 (s, CH(*C*H$_3$)$_2$), 18.8 (s, CH(*C*H$_3$)$_2$), 18.5 (s, CH(CH$_3$)$_2$), 17.2 (s, CH(CH$_3$)$_2$). ^{31}P{^{1}H} NMR (δ, CD_2Cl_2, 20 °C): 147.1. IR (ATR, cm^{-1}): 1902 (ν_{CO}). ESI-MS (m/z, EtOH); pos. ion: 426.1 [M − Br]$^+$, 398.2 [M − Br − CO]$^+$.

[Fe(PNP^{Me}-*i*Pr)(H)(CO)Br] (2b). This complex was prepared analogously to **2a** using **1b** (300 mg, 0.81 mmol), $FeBr_2$ (175 mg, 0.81 mg), and Na[HBEt$_3$] (0.89 mL, 1 M in toluene, 0.89 mmol) as starting materials. The product was obtained as a mixture of two isomers in a 2.7:1 ratio (**2b**, **2b**′). Yield: 276 mg (64%) of a red-orange powder. Anal. Calcd for $C_{20}H_{38}BrFeN_3OP_2$: C, 44.96; H, 7.17; N, 7.87. Found: C, 44.86; H, 7.22; N, 7.07. **2b:** ^{1}H NMR (δ, CD_2Cl_2, 20 °C): 7.44 (t, J = 8.3 Hz, 1H, py^4), 6.02 (d, J = 8.3 Hz, 2H, py^{3,5}), 3.10 (s, 3H, NC*H*$_3$), 2.80 (m, 2H, C*H*(CH$_3$)$_2$), 2.55 (m, 2H, C*H*(CH$_3$)$_2$), 1.72 (dd, J = 7.3 Hz, J = 16.6, 6H, CH(C*H*$_3$)$_2$), 1.60 (dd, J = 7.3 Hz, J = 14.5, 6H, CH(C*H*$_3$)$_2$), 1.22 (dd, J = 7.3 Hz, J = 16.8, 6H, CH(C*H*$_3$)$_2$), 0.83 (dd, J = 7.0 Hz, J = 14.1, 6H, CH(C*H*$_3$)$_2$), −21.84 (t, $^2J_{HP}$ = 57.5, 1H, Fe*H*). ^{13}C{^{1}H} NMR (δ, CD_2Cl_2, 20 °C): 222.7 (t, $^2J_{CP}$ = 22.4 Hz, CO), 162.6 (t, $^2J_{CP}$ = 11.4 Hz, py^{2,6}), 138.9 (s, py^4), 96.6 (s, py^{3,5}), 34.0 (s, NCH$_3$), 33.6 (t, $^1J_{CP}$ = 9.3 Hz, CH(CH$_3$)$_2$), 31.2 (t, $^1J_{CP}$ = 14.8 Hz, CH(CH$_3$)$_2$), 21.7 (s, CH(CH$_3$)$_2$), 20.3 (t, $^2J_{CP}$ = 3.6 Hz, CH(CH$_3$)$_2$), 18.3 (s, CH(CH$_3$)$_2$), 17.8 (t, $^2J_{CP}$ = 5.0 Hz CH(CH$_3$)$_2$). ^{31}P{^{1}H} NMR (δ, CD_2Cl_2, 20 °C): 164.0 (s). IR (ATR, cm^{-1}): 1903 (ν_{CO}). **2b′:** ^{1}H NMR (δ, CD_2Cl_2, 20 °C): 7.13 (t, J = 8.2 Hz, 1H, py^4), 5.65 (d, J = 8.2 Hz, 2H, py^{3,5}), 3.04 (m, 2H, C*H*(CH$_3$)$_2$), 2.97 (s, 3H, NC*H*$_3$), 2.83 (m, 2H, C*H*(CH$_3$)$_2$), 1.61 (dd, J = 7.4 Hz, J = 16.1, 6H, CH(C*H*$_3$)$_2$), 1.54 (dd, J = 7.0 Hz, J = 14.3, 6H, CH(C*H*$_3$)$_2$), 1.50 (dd, J = 7.4 Hz, J = 16.3, 6H, CH(C*H*$_3$)$_2$), 1.29 (dd, J = 7.0 Hz, J = 14.3, 6H, CH(C*H*$_3$)$_2$), −1.08 (t, $^2J_{HP}$ = 57.1, 1H, Fe*H*). ^{13}C{^{1}H} NMR (δ, CD_2Cl_2, 20 °C): 217.1 (t, $^2J_{CP}$ = 13.0 Hz, CO), 163.5 (t, $^2J_{CP}$ = 9.8 Hz, py^{2,6}), 137.0 (s, py^4), 95.4 (s, py^{3,5}), 33.3 (s, NCH$_3$), 31.6 (t, $^1J_{CP}$ = 12.9 Hz, CH(CH$_3$)$_2$), 31.3 (t, $^1J_{CP}$ = 8.6 Hz, CH(CH$_3$)$_2$), 19.2 (t, $^2J_{CP}$ = 3.7 Hz, CH(CH$_3$)$_2$), 18.8 (s, CH(CH$_3$)$_2$), 18.7 (t, $^2J_{CP}$ = 2.3 Hz, CH(CH$_3$)$_2$), 18.3 (s, CH(CH$_3$)$_2$). ^{31}P{^{1}H} NMR (δ, CD_2Cl_2, 20 °C): 161.6. IR (ATR, cm^{-1}): 1903 (ν_{CO}).

dx.doi.org/10.1021/om5009814 | *Organometallics* 2014, 33, 6905−6914

[Fe(PNP^{H,Me}-*i*Pr)(H)(CO)Br] (2c). This complex was prepared analogously to **2a** using **1c** (300 mg, 0.84 mmol), $FeBr_2$ (181 mg, 0.84 mg), and Na[$HBEt_3$] (0.92 mL, 1 M in toluene, 0.92 mmol) as starting materials. Yield: 275 mg (63%) of an orange powder. Anal. Calcd for $C_{19}H_{36}BrFeN_3OP_2$: C, 43.87; H, 6.98; N, 8.08. Found: C, 43.59; H, 7.19; N, 7.96. ^{1}H NMR (δ, CD_2Cl_2, 20 °C): 7.31 (t, J = 7.8 Hz, 1H, py^4), 6.22 (d, J = 7.8 Hz, 1H, py^{3,5}), 5.91 (d, J = 7.8 Hz, 1H, py^{3,5}), 5.61 (bs, 1H, N*H*), 2.80 (m, 1H, C*H*(CH_3)$_2$), 3.07 (d, J = 3.1 Hz, 3H, NCH_3), 2.75 (m, 1H, C*H*(CH_3)$_2$), 2.53 (m, 2H, C*H*(CH_3)$_2$), 1.72 (dd, J = 6.9 Hz, J = 17.4, 3H, CH(CH_3)$_2$), 1.55 (dd, J = 7.3 Hz, J = 13.6, 3H, CH(CH_3)$_2$), 1.52 (dd, J = 7.8 Hz, J = 9.5, 3H, CH(CH_3)$_2$), 1.44 (dd, J = 7.1 Hz, J = 10.7, 3H, CH(CH_3)$_2$), 1.26 (dd, J = 6.8 Hz, J = 17.0, 3H, CH(CH_3)$_2$), 1.18 (dd, J = 6.9 Hz, J = 17.4, 3H, CH(CH_3)$_2$), 0.94 (dd, J = 6.7 Hz, J = 14.4, 3H, CH(CH_3)$_2$), 0.88 (dd, J = 6.7 Hz, J = 14.4, 3H, CH(CH_3)$_2$), −21.64 (t, $^2J_{HP}$ = 57.2, 1H, Fe*H*). ^{13}C{^{1}H} NMR (δ, CD_2Cl_2, 20 °C): 222.5 (br, *C*O), 162.4 (br, py^{2,6}), 161.0 (br, py^{2,6}), 138.9 (s, py^4), 98.2 (d, $^3J_{CP}$ = 6.8 Hz, py^{3,5}), 95.7 (d, $^3J_{CP}$ = 6.8 Hz, py^{3,5}), 33.5 (d, $^1J_{CP}$ = 21.7 Hz, *C*H(CH_3)$_2$), 33.4 (d, $^2J_{CP}$ = 12.1 Hz, N*C*H_3), 31.7 (d, $^1J_{CP}$ = 28.6 Hz, *C*H(CH_3)$_2$), 29.0 (d, $^1J_{CP}$ = 22.8 Hz, *C*H(CH_3)$_2$), 27.1 (d, $^1J_{CP}$ = 24.1 Hz, *C*H(CH_3)$_2$), 21.1 (s, CH(*C*H_3)$_2$), 20.4 (d, $^2J_{CP}$ = 8.8 Hz, CH(*C*H_3)$_2$), 19.5 (d, $^2J_{CP}$ = 8.8 Hz, CH(*C*H_3)$_2$), 18.7 (d, $^2J_{CP}$ = 10.1 Hz, CH(*C*H_3)$_2$), 18.5 (s, CH(*C*H_3)$_2$), 18.3 (s, CH(*C*H_3)$_2$), 18.0 (d, $^2J_{CP}$ = 9.4 Hz, CH(*C*H_3)$_2$), 17.1 (d, $^2J_{CP}$ = 7.9 Hz, CH(*C*H_3)$_2$). ^{31}P{^{1}H} NMR (δ, CD_2Cl_2, 20 °C): 165.0 (d, J_{PP} = 145.1 Hz), 147.2 (d, J_{PP} = 145.1 Hz). IR (ATR, cm^{-1}): 1901 (ν_{CO}).

[Fe(PNP-*i*Pr)(H)(CO)(CH_3CN)]BF_4 (3b). To a solution of **2a** (150 mg, 0.30 mmol) in CH_3CN (10 mL) was added $AgBF_4$ (58 mg, 0.30 mmol). After stirring for 5 min at room temperature, the precipitate was filtered off and the solvent was removed under reduced pressure. The product was washed twice with diethyl ether and dried under vacuum to afford a pale green powder. Yield: 148 mg (89%). Anal. Calcd for $C_{20}H_{37}BF_4FeN_4OP_2$: C, 43.35; H, 6.73; N, 10.11. Found: C, 43.28; H, 6.78; N, 10.02. ^{1}H NMR (δ, acetone-d_6, 20 °C): 7.64 (s, 2H, N*H*), 7.63 (t, J = 7.9 Hz, 1H, py^4), 6.33 (d, J = 7.9 Hz, 2H, py^{3,5}), 2.67 (m, 4H, C*H*(CH_3)$_2$), 2.40 (s, 3H, CH_3CN), 1.53 (m, 12H, CH(CH_3)$_2$), 1.22 (dd, J = 7.1 Hz, J = 17.4 Hz, 6H, CH(CH_3)$_2$), 1.06 (dd, J = 6.9 Hz, J = 14.8 Hz, 6H, CH(CH_3)$_2$), −18.55 (t, $^2J_{HP}$ = 53.3 Hz, 1H, Fe*H*). ^{13}C{^{1}H} NMR (δ, CD_2Cl_2, 20 °C): 218.7 (t, $^2J_{CP}$ = 21.7 Hz, *C*O), 161.1 (t, $^2J_{CP}$ = 9.0 Hz, py^{2,6}), 140.3 (s, py^4), 127.2 (s, CH_3*C*N), 98.9 (s, py^{3,5}), 31.0 (t, $^1J_{CP}$ = 10.2 Hz, *C*H(CH_3)$_2$), 29.8 (t, $^1J_{CP}$ = 15.4 Hz, *C*H(CH_3)$_2$), 19.4 (s, CH(*C*H_3)$_2$), 18.2 (s, CH(*C*H_3)$_2$), 4.5 (s, CH_3*C*N). ^{31}P{^{1}H} NMR (δ, CD_2Cl_2, 20 °C): 145.6). IR (ATR, cm^{-1}): 1929 (ν_{CO}). ESI-MS (*m*/*z*, EtOH); pos. ion: 426.1 [M − CH_3CN]$^+$, 398.1 [M − CH_3CN − CO]$^+$. Crystals suitable for X-ray crystallography were grown with Br^- as counterion (analogously prepared without the addition of a silver salt as halide scavenger) by slow evaporation of a CH_3CN/THF (1:1) solution.

[Fe(PNP-*i*Pr)(H)(CO)(py)]BF_4 (3c). To a solution of **2a** (150 mg, 0.30 mmol) in CH_3OH (8 mL) was added pyridine (36 μL, 0.45 mmol). After stirring for 5 min at room temperature, $AgBF_4$ (58 mg, 0.30 mmol) was added and the reaction mixture was stirred for an additional 5 min. The dark precipitate was filtered off, and the solvent was removed under reduced pressure. The residue was washed twice with diethyl ether and dried under vacuum to afford a yellow powder. Yield: 150 mg (83%). Anal. Calcd for $C_{23}H_{39}BF_4FeN_4OP_2$: C, 46.65; H, 6.64; N, 9.46. Found: C, 47.07; H, 6.95; N, 9.29. ^{1}H NMR (δ, MeOH-d_4, 20 °C): 10.00−6.55 (broad and unresolved signals, 4H, pyridine-*H*^{2,3,5,6}), 7.77 (t, J = 7.6 Hz, 1H, pyridine-*H*^{4}), 7.46 (t, J = 8.0 Hz, 1H, py^4), 6.34 (d, J = 8.0 Hz, 2H, py^{3,5}), 2.50 (m, 2H, C*H*(CH_3)$_2$), 1.89 (m, 2H, C*H*(CH_3)$_2$), 1.28−1.19 (m, 12H, CH(CH_3)$_2$), 1.07 (dd, J = 6.8 Hz, J = 14.3, 6H, CH(CH_3)$_2$), 0.93 (dd, J = 7.5 Hz, J = 15.6, 6H, CH(CH_3)$_2$), −20.08 (t, $^2J_{HP}$ = 52.9 Hz, 1H, Fe*H*). ^{13}C{^{1}H} NMR (δ, MeOH-d_4, 20 °C): 220.3 (t, $^2J_{CP}$ = 22.8 Hz, *C*O), 163.0 (t, $^2J_{CP}$ = 9.0 Hz, py^{2,6}), 141.0 (d, $^3J_{CP}$ = 13.6 Hz, pyridine-*C*^{2,6}), 138.8 (s, pyridine-*C*^{4}), 138.5 (s, py^4), 126.9 (s, pyridine-*C*^{3,5}), 99.3−98.6 (unresolved signal), 30.3 (t, $^1J_{CP}$ = 16.3 Hz, *C*H(CH_3)$_2$), 18.9 (s, CH(*C*H_3)$_2$), 18.7 (s, CH(*C*H_3)$_2$), 18.3 (s, CH(*C*H_3)$_2$), 17.5 (s, CH(*C*H_3)$_2$). ^{31}P{^{1}H} NMR (δ, MeOH-d_4, 20 °C): 142.3. IR (ATR, cm^{-1}): 1906 (ν_{CO}). ESI-MS (*m*/*z*, EtOH); pos. ion: 505.1 [M]$^+$, 426.1 [M − C_5H_5N]$^+$.

[Fe(PNP-*i*Pr)(H)(CO)(PMe_3)]BF_4 (3d). To a solution of **2a** (150 mg, 0.30 mmol) in CH_3OH (8 mL) was added PMe_3 (47 mL, 0.45 mmol). After stirring for 5 min at room temperature, $AgBF_4$ (58 mg, 0.30 mmol) was added and the reaction mixture was stirred for an additional 5 min. The dark precipitate was filtered off, and the solvent of the filtrate was removed *in vacuo*. The residue was washed twice with *n*-pentane and dried under high vacuum to give an off-white powder. Yield: 172 mg (97%). Anal. Calcd for $C_{21}H_{43}BF_4FeN_3OP_3$: C, 42.81; H, 7.36; N, 7.13. Found: C, 42.94; H, 7.58; N, 7.58. ^{1}H NMR (δ, MeOH-d_4, 20 °C): 7.31 (t, J = 7.8 Hz, 1H, py^4), 6.22 (d, J = 7.8 Hz, 2H, py^{3,5}), 2.73 (m, 2H, C*H*(CH_3)$_2$), 2.62 (m, 2H, C*H*(CH_3)$_2$), 1.58−1.45 (m, 12H, CH(CH_3)$_2$), 1.25 (m, 6H, CH(CH_3)$_2$), 1.23 (d, J = 7.2 Hz, 3H, P(CH_3)$_3$), 0.99 (dd, J = 6.8 Hz, J = 14.7, 6H, CH(CH_3)$_2$), −11.09 (dt, $^2J_{HP}$ = 35.7 Hz, $^2J_{HP}$ = 60.7 Hz, 1H, Fe*H*). ^{13}C{^{1}H} NMR (δ, MeOH-d_4, 20 °C): 220.5 (dt, J_{CP} = 15.2 Hz, J_{CP} = 23.2 Hz, *C*O), 162.0 (t, J_{CP} = 8.4 Hz, py^{2,6}), 140.7 (s, py^4), 98.9 (s, py^{3,5}), 34.7 (t, J_{CP} = 11.7 Hz, *C*H(CH_3)$_2$), 28.7 (dt, J_{CP} = 8.0 Hz, J_{CP} = 14.8 Hz, *C*H(CH_3)$_2$), 19.8 (t, J_{CP} = 4.6 Hz, CH(*C*H_3)$_2$), 19.0 (t, J_{CP} = 4.6 Hz, CH(*C*H_3)$_2$), 18.8 (d, J_{CP} = 23.2 Hz, P(*C*H_3)$_3$), 17.9 (s, CH(*C*H_3)$_2$), 17.4 (bs, CH(*C*H_3)$_2$). ^{31}P{^{1}H} NMR (δ, MeOH-d_4, 20 °C): 147.3 (d, J = 25.6 Hz, 2P, *Pi*Pr$_2$), 2.9 (t, J = 25.6 Hz, *P*Me$_3$). IR (ATR, cm^{-1}): 1910 (ν_{CO}). ESI-MS (*m*/*z*, EtOH); pos. ion: 502.2 [M]$^+$, 426.1 [M − PMe_3]$^+$.

[Fe(PNP-*i*Pr)(H)(CO)(κ^1-*N*-SCN)] (3e). To a solution of **2a** (150 mg, 0.30 mmol) in THF (10 mL) was added NaSCN (27 mg, 0.33 mmol). After stirring for 1 h at room temperature, the solution was filtered and the solvent was removed under reduced pressure. The product was washed twice with diethyl ether and dried under vacuum to afford an off-white powder. Yield: 136 mg (93%). Anal. Calcd for $C_{19}H_{34}FeN_4OP_2S$: C, 47.12; H, 7.08; N, 11.57. Found: C, 47.18; H, 7.13; N, 11.42. ^{1}H NMR (δ, DMSO-d_6, 20 °C): 8.26 (s, 2H, N*H*), 7.26 (t, J = 7.9 Hz, 1H, py^4), 6.13 (d, J = 7.9 Hz, 2H, py^{3,5}), 2.48 (m, 2H, C*H*(CH_3)$_2$), 2.41 (m, 2H, C*H*(CH_3)$_2$), 1.44 (m, 6H, CH(CH_3)$_2$), 1.38 (m, 6H, CH(CH_3)$_2$), 1.12 (m, 6H, CH(CH_3)$_2$), 0.95 (m, 6H, CH(CH_3)$_2$), −19.84 (t, $^2J_{HP}$ = 52.1 Hz, 1H, Fe*H*). ^{13}C{^{1}H} NMR (δ, DMSO-d_6, 20 °C): 220.7 (t, $^2J_{CP}$ = 24.1 Hz, *C*O), 161.0 (t, $^2J_{CP}$ = 9.6 Hz, py^{2,6}), 138.7 (s, py^4), 137.4 (d, $^3J_{CP}$ = 5.4 Hz, *S*CN), 96.6 (s, py^{3,5}), 29.5 (t, $^1J_{CP}$ = 10.6 Hz, *C*H(CH_3)$_2$), 27.8 (t, $^1J_{CP}$ = 14.9 Hz, *C*H(CH_3)$_2$), 18.8 (s, CH(*C*H_3)$_2$), 17.9 (s, CH(*C*H_3)$_2$), 17.8 (s, CH(*C*H_3)$_2$), 17.4 (s, CH(*C*H_3)$_2$). ^{31}P{^{1}H} NMR (δ, CD_2Cl_2, 20 °C): 146.6. IR (ATR, cm^{-1}): 2074 (ν_{NCS}), 1921 (ν_{CO}). ESI-MS (*m*/*z*, EtOH, NaCl); pos. ion: 507.1 [M + Na]$^+$, 426.1 [M − SCN]$^+$, 398.2 [M − SCN − CO]$^+$.

[Fe(PNP-*i*Pr)(H)(CO)(κ^1-BH_4)] (3g). *Method A.* To a solution of **2a** (200 mg, 0.40 mmol) in THF (24 mL) was added sodium borohydride (76 mg, 2.00 mmol). After stirring for 6 h at room temperature, the solution was filtered and the solvent was removed under reduced pressure. The residue was dissolved in THF (1.0 mL), and the product was precipitated by addition of *n*-pentane. The bright yellow powder was washed twice with *n*-pentane and dried under vacuum. Yield: 132 mg (75%).

Method B. To a suspension of [Fe(PNP-*i*Pr)(CO)$(Br)_2$] (200 mg, 0.40 mmol) in EtOH (10 mL) was added sodium borohydride (65 mg, 1.71 mmol). An immediate gas evolution took place, and the initially blue suspension turned into a dark orange solution within 5 min. After stirring the reaction mixture for 30 min, all volatiles were removed under reduced pressure. The residue was dissolved in dichloromethane (10 mL), the resulting solution was filtered, and the solvent was removed under vacuum. Yield: 136 mg (91%). Anal. Calcd for $C_{18}H_{38}BFeN_3OP_2$: C, 49.01; H, 8.68; N, 9.53. Found: C, 48.95; H, 8.61; N, 9.77. ^{1}H NMR (δ, CD_2Cl_2, 20 °C): 7.17 (t, J = 7.9 Hz, 1H, py^4), 6.13 (d, J = 7.9 Hz, 2H, py^{3,5}), 5.43 (bs, 2H, N*H*), 3.01 (m, 2H, C*H*(CH_3)$_2$), 2.50 (m, 2H, C*H*(CH_3)$_2$), 1.50 (dd, J = 7.6 Hz, J = 17.7 Hz, 6H, CH(CH_3)$_2$), 1.42 (dd, J = 7.0 Hz, J = 12.5 Hz, 6H, CH(CH_3)$_2$), 1.22 (dd, J = 7.0 Hz, J = 17.4 Hz, 6H, CH(CH_3)$_2$), 1.05 (dd, J = 6.7 Hz, J = 14.4 Hz, 6H, CH(CH_3)$_2$), −3.61 (br, 4H, BH_4), −18.12 (t, $^2J_{HP}$ = 52.1 Hz, 1H, Fe*H*). ^{13}C{^{1}H} NMR (δ, CD_2Cl_2, 20 °C): 160.8 (t, $^2J_{CP}$ = 9.1 Hz, py^{2,6}), 138.5 (s, py^4), 97.3 (s, py^{3,5}), 31.4

dx.doi.org/10.1021/om5009814 | *Organometallics* 2014, 33, 6905−6914

(t, $^1J_{CP}$ = 10.6 Hz, $CH(CH_3)_2$), 27.8 (t, $^1J_{CP}$ = 13.2 Hz, $CH(CH_3)_2$), 19.5 (t, $^2J_{CP}$ = 3.8 Hz, $CH(CH_3)_2$), 18.6 (t, $^2J_{CP}$ = 4.6 Hz, $CH(CH_3)_2$), 18.4 (s, $CH(CH_3)_2$), 17.4 (s, $CH(CH_3)_2$), the CO resonance could not be observed. $^{31}P\{^1H\}$ NMR (δ, CD_2Cl_2, 20 °C): 151.2. IR (ATR, cm^{-1}): 1911 (ν_{CO}). ESI-MS (m/z, EtOH); pos. ion: 426.1 $[M - BH_4]^+$, 398.1 $[M - BH_4 - CO]^+$.

X-ray Structure Determination. X-ray diffraction data of **2a**·CD_2Cl_2, **3b**, **3c**, **3e**, and **3f** were collected at T = 100 K (**3f**: T = 200 K due to a phase transition at lower temperatures) in a dry stream of nitrogen on Bruker Kappa APEX II diffractometer systems using graphite-monochromatized Mo Kα radiation (λ = 0.710 73 Å) and fine sliced φ- and ω-scans. Data of **3d** were collected at T = 185 K on a Bruker SMART APEX diffractometer using ω-scans. Data were reduced to intensity values with SAINT, and an absorption correction was applied with the multiscan approach implemented in SADABS.[23] The structures were solved by charge flipping using SUPERFLIP[24] and refined against F with JANA2006.[25] Non-hydrogen atoms were refined anisotropically. The H atoms connected to C atoms were placed in calculated positions and thereafter refined as riding on the parent atoms. H atoms connected to N, B, and Fe atoms were located in difference Fourier maps. The Fe−H distances were restrained. The N−H distances were restrained in **2a**·CD_2Cl_2 and **3d**, whereas the N−H atoms in the remaining models were freely refined. In **3f**, the B−H distances were restrained to 1.000(1) Å. Molecular graphics were generated with the program MERCURY.[26] Crystal data and experimental details are given in Tables S1 and S2.

Computational Details. All calculations were performed using the Gaussian 09 software package[27] on the Phoenix Linux Cluster of the Vienna University of Technology. The optimized geometries were obtained with the B3LYP functional.[28] That functional includes a mixture of Hartree−Fock[29] exchange with DFT[19] exchange−correlation, given by Becke's three-parameter functional with the Lee, Yang, and Parr correlation functional, which includes both local and nonlocal terms. The basis set used for the geometry optimizations (basis b1) consisted of the Stuttgart/Dresden ECP (SDD) basis set[30] to describe the electrons of iron and a standard 6-31G(d,p) basis set[31] for all other atoms. Transition-state optimizations were performed with the Synchronous Transit-Guided Quasi-Newton Method (STQN) developed by Schlegel et al.,[32] following extensive searches of the potential energy surface. Frequency calculations were performed to confirm the nature of the stationary points, yielding one imaginary frequency for the transition states and none for the minima. Each transition state was further confirmed by following its vibrational mode downhill on both sides and obtaining the minima presented on the energy profiles. Atomic charges were obtained by means of a natural population analysis (NPA).[33] The electronic energies (E_{b1}) obtained at the B3LYP/b1 level of theory were converted to free energy at 298.15 K and 1 atm (G_{b1}) by using zero-point energy and thermal energy corrections based on structural and vibration frequency data calculated at the same level.

Single-point energy calculations were performed using the M06 functional and a standard 6-311++G(d,p) basis set,[34] on the geometries optimized at the B3LYP/b1 level. The M06 functional is a hybrid meta-GGA functional developed by Truhlar and Zhao,[35] and it was shown to perform very well for the kinetics of transition metal molecules, providing a good description of weak and long-range interactions.[36] Solvent effects (ethanol) were considered in the M06/6-311++G(d,p)//B3LYP/b1 energy calculations using the polarizable continuum model (PCM) initially devised by Tomasi and co-workers[37] with radii and nonelectrostatic terms of the SMD solvation model, developed by Truhler et al.[38] The free energy values presented (G_{b2}^{soln}) were derived from the electronic energy values obtained at the M06/6-311++G(d,p)//B3LYP/b1 level, including solvent effects (E_{b2}^{soln}), according to the following expression: $G_{b2}^{soln} = E_{b2}^{soln} + G_{b1} - E_{b1}$.

■ ASSOCIATED CONTENT

Supporting Information

Coordinates of the optimized structures, ^1H, $^{13}C\{^1H\}$, and $^{31}P\{^1H\}$ NMR spectra of all complexes, crystallographic data and technical details in CIF format for **2a**, **3b**, **3e** (CCDC 1010393−1010395) and **3c**, **3d**, **3g** (CCDC 1023528−1023530). This material is available free of charge via the Internet at http://pubs.acs.org.

■ AUTHOR INFORMATION

Corresponding Author

*E-mail: kkirch@mail.tuwien.ac.at.

Notes

The authors declare no competing financial interest.

■ ACKNOWLEDGMENTS

Financial support by the Austrian Science Fund (FWF) is gratefully acknowledged (Project No. P24583-N28), and L.F.V. and L.P.F. acknowledge Fundação para a Ciência e Tecnologia, Projecto Estratégico - PEst-OE/QUI/UI0100/2013 and PEst-OE/FIS/UI0261/2014, respectively. The X-ray center of the Vienna University of Technology is acknowledged for financial support and for providing access to the single-crystal diffractometer.

■ REFERENCES

(1) (a) Noyori, R.; Ohkuma, T. *Angew. Chem., Int. Ed.* **2001**, *40*, 40−73. (b) Noyori, R. *Angew. Chem., Int. Ed.* **2013**, *52*, 79−92. (c) de Vries, J. G., Elsevier, C. J., Eds. *Handbook of Homogeneous Hydrogenation*; Wiley-VCH: Weinheim, 2007. (d) Johnson, N. B.; Lennon, I. C.; Moran, P. H.; Ramsden, J. A. *Acc. Chem. Res.* **2007**, *40*, 1291−1299. (e) Dub, P. A.; Ikariya, T. *ACS Catal.* **2012**, *2*, 1718−1741.

(2) For recent reviews on iron-catalyzed reaction see: (a) Morris, R. H. *Chem. Soc. Rev.* **2009**, *38*, 2282−2291. (b) Enthaler, S.; Junge, K.; Beller, M. *Angew. Chem., Int. Ed.* **2008**, *47*, 3317−3321. (c) Gaillard, S.; Renaud, J.-L. *ChemSusChem* **2008**, *1*, 505−509. (d) Bauer, G.; Kirchner, K. A. *Angew. Chem., Int. Ed.* **2011**, *50*, 5798−5800. (e) Bullock, R. M. *Science* **2013**, *342*, 1054−1055. (f) Sues, P. E.; Demmans, Z.; Morris, R. H. *Dalton Trans.* **2014**, *43*, 7650−7667.

(3) (a) Casey, C. P.; Guan, H. *J. Am. Chem. Soc.* **2007**, *129*, 5816−5817. (b) Casey, C. P.; Guan, H. *J. Am. Chem. Soc.* **2009**, *131*, 2499−2507.

(4) (a) Langer, R.; Leitus, G.; Ben-David, Y.; Milstein, D. *Angew. Chem., Int. Ed.* **2011**, *50*, 2120−2124. (b) Langer, R.; Diskin-Posner, Y.; Leitus, G.; Shimon, L. J.; Ben-David, Y.; Milstein, D. *Angew. Chem., Int. Ed.* **2011**, *50*, 9948−9952. (c) Langer, R.; Iron, M. A.; Konstantinovski, L.; Diskin-Posner, Y.; Leitus, G.; Ben-David, Y.; Milstein, D. *Chem.—Eur. J.* **2012**, *18*, 7196−7209. (d) Zell, T.; Butschke, B.; Ben-David, Y.; Milstein, D. *Chem.—Eur. J.* **2013**, *19*, 8068−8072. (e) Zell, T.; Ben-David, Y.; Milstein, D. *Angew. Chem., Int. Ed.* **2014**, *53*, 4685−4689.

(5) Berkessel, A.; Reichau, S.; von der Höh, A.; Leconte, N.; Neudörfl, J.-M. *Organometallics* **2011**, *30*, 3880−3887.

(6) (a) Sui-Seng, C.; Freutel, F.; Lough, A. J.; Morris, R. H. *Angew. Chem., Int. Ed.* **2008**, *47*, 940−943. (b) Sui-Seng, C.; Haque, F. N.; Hadzovic, A.; Pütz, A.-M.; Reuss, V.; Meyer, N.; Lough, A. J.; Zimmer-De Iuliis, M.; Morris, R. H. *Inorg. Chem.* **2009**, *48*, 735−743. (c) Lagaditis, P. O.; Sues, P. E.; Sonnenberg, J. F.; Wan, K. Y.; Lough, A. J.; Morris, R. H. *J. Am. Chem. Soc.* **2014**, *136*, 1367−1380. (d) Zuo, W.; Tauer, S.; Prokopchuk, D. E.; Morris, R. H. *Organometallics* **2014**, *33*, 5791−5801. (e) Sonnenberg, J. F.; Lough, A. J.; Morris, R. H. *Organometallics* **2014**, in press.

(7) (a) Tlili, A.; Schranck, J.; Neumann, H.; Beller, M. *Chem.—Eur. J.* **2012**, *18*, 15935−15939. (b) Fleischer, S.; Zhou, S.; Junge, K.; Beller, M. *Angew. Chem., Int. Ed.* **2013**, *52*, 5120−5124.

(8) (a) Crabtree, R. H. *New J. Chem.* **2011**, *35*, 18−23. (b) Grützmacher, H. *Angew. Chem., Int. Ed.* **2008**, *47*, 1814−1818. (c) van der Vlugt, J. I.; Reek, J. N. H. *Angew. Chem., Int. Ed.* **2009**, *48*, 8832−8846.
(9) (a) Gunanathan, C.; Milstein, D. *Acc. Chem. Res.* **2011**, *44*, 588−602. (b) Gunanathan, C.; Milstein, D. *Top. Organomet. Chem.* **2011**, *37*, 55−84. (c) Poverenov, E.; Milstein, D. *Top. Organomet. Chem.* **2013**, *40*, 21−47. (d) Chang, Y.-H.; Nakajima, Y.; Tanaka, H.; Yoshizawa, K.; Ozawa, F. *J. Am. Chem. Soc.* **2013**, *135*, 11791−11794.
(10) (a) Bichler, B.; Glatz, M.; Stöger, B.; Mereiter, K.; Veiros, L. F.; Kirchner, K. *Dalton Trans.* **2014**, *43*, 14517−15419. (b) de Aguiar, S. R. M. M.; Öztopcu, Ö.; Stöger, B.; Mereiter, K.; Veiros, L. F.; Pittenauer, E.; Allmaier, G.; Kirchner, K. *Dalton Trans.* **2014**, *43*, 14669−14679.
(11) Bichler, B.; Holzhacker, C.; Stöger, B.; Puchberger, M.; Veiros, L. F.; Kirchner, K. *Organometallics* **2013**, *32*, 4114−4121.
(12) Wienhöfer, G.; Westerhaus, F. A.; Junge, K.; Ludwig, R.; Beller, M. *Chem.—Eur. J.* **2013**, *19*, 7701−7707.
(13) Benito-Garagorri, D.; Alves, L. G.; Puchberger, M.; Mereiter, K.; Veiros, L. F.; Calhorda, M. J.; Carvalho, M. D.; Ferreira, L. P.; Godinho, M.; Kirchner, K. *Organometallics* **2009**, *28*, 6902−6914.
(14) Sandoval, C. A.; Ohkuma, T.; Muniz, K.; Noyori, R. *J. Am. Chem. Soc.* **2003**, *125*, 13490−13503.
(15) Bielinski, E. A.; Lagaditis, P. O.; Zhang, Y.; Mercado, B. Q.; Würtele, C.; Bernskoetter, W. H.; Hazari, N.; Schneider, S. *J. Am. Chem. Soc.* **2014**, *136*, 10234−10237.
(16) Chakraborty, S.; Brennessel, W. W.; Jones, W. D. *J. Am. Chem. Soc.* **2014**, *136*, 8564−8567.
(17) Yang, Y. *Inorg. Chem.* **2011**, *50*, 12836−12843.
(18) Chakraborty, S.; Dai, H.; Bhattacharya, P.; Fairweather, N. T.; Gibson, M. S.; Krause, J. A.; Guan, H. *J. Am. Chem. Soc.* **2014**, *136*, 7869−7872.
(19) Parr, R. G.; Yang, W. *Density Functional Theory of Atoms and Molecules*; Oxford University Press: New York, 1989.
(20) Perrin, D. D.; Armarego, W. L. F. *Purification of Laboratory Chemicals*, 3rd ed.; Pergamon: New York, 1988.
(21) Benito-Garagorri, D.; Becker, E.; Wiedermann, J.; Lackner, W.; Pollak, M.; Mereiter, K.; Kisala, J.; Kirchner, K. *Organometallics* **2006**, *25*, 1900−1913.
(22) Öztopcu, Ö.; Holzhacker, C.; Puchberger, M.; Weil, M.; Mereiter, K.; Veiros, L. F.; Kirchner, K. *Organometallics* **2013**, *32*, 3042−3052.
(23) Bruker computer programs: *APEX2*, *SAINT*, and *SADABS*; Bruker AXS Inc.: Madison, WI, 2012.
(24) Palatinus, L.; Chapuis, G. *J. Appl. Crystallogr.* **2007**, *40*, 786−790.
(25) Petříček, V.; Dušek, M.; Palatinus, L. *JANA2006, the crystallographic computing system*; Institute of Physics: Praha, Czeck Republic, 2006.
(26) Macrae, C. F.; Edgington, P. R.; McCabe, P.; Pidcock, E.; Shields, G. P.; Taylor, R.; Towler, M.; van de Streek, J. *J. Appl. Crystallogr.* **2006**, *39*, 453.
(27) Frisch, M. J.; Trucks, G. W.; Schlegel, H. B.; Scuseria, G. E.; Robb, M. A.; Cheeseman, J. R.; Scalmani, G.; Barone, V.; Mennucci, B.; Petersson, G. A.; Nakatsuji, H.; Caricato, M.; Li, X.; Hratchian, H. P.; Izmaylov, A. F.; Bloino, J.; Zheng, G.; Sonnenberg, J. L.; Hada, M.; Ehara, M.; Toyota, K.; Fukuda, R.; Hasegawa, J.; Ishida, M.; Nakajima, T.; Honda, Y.; Kitao, O.; Nakai, H.; Vreven, T.; Montgomery, J. A., Jr.; Peralta, J. E.; Ogliaro, F.; Bearpark, M.; Heyd, J. J.; Brothers, E.; Kudin, K. N.; Staroverov, V. N.; Kobayashi, R.; Normand, J.; Raghavachari, K.; Rendell, A.; Burant, J. C.; Iyengar, S. S.; Tomasi, J.; Cossi, M.; Rega, N.; Millam, J. M.; Klene, M.; Knox, J. E.; Cross, J. B.; Bakken, V.; Adamo, C.; Jaramillo, J.; Gomperts, R.; Stratmann, R. E.; Yazyev, O.; Austin, A. J.; Cammi, R.; Pomelli, C.; Ochterski, J. W.; Martin, R. L.; Morokuma, K.; Zakrzewski, V. G.; Voth, G. A.; Salvador, P.; Dannenberg, J. J.; Dapprich, S.; Daniels, A. D.; Farkas, Ö.; Foresman, J. B.; Ortiz, J. V.; Cioslowski, J.; Fox, D. J. *Gaussian 09*, Revision A.02; Gaussian, Inc.: Wallingford, CT, 2009.
(28) (a) Becke, A. D. *J. Chem. Phys.* **1993**, *98*, 5648−5652. (b) Miehlich, B.; Savin, A.; Stoll, H.; Preuss, H. *Chem. Phys. Lett.* **1989**, *157*, 200−206. (c) Lee, C.; Yang, W.; Parr, G. *Phys. Rev. B* **1988**, *37*, 785−789.
(29) Hehre, W. J.; Radom, L.; Schleyer, P. v. R.; Pople, J. A. *Ab Initio Molecular Orbital Theory*; John Wiley & Sons: New York, 1986.
(30) (a) Haeusermann, U.; Dolg, M.; Stoll, H.; Preuss, H. *Mol. Phys.* **1993**, *78*, 1211−1224. (b) Kuechle, W.; Dolg, M.; Stoll, H.; Preuss, H. *J. Chem. Phys.* **1994**, *100*, 7535−7542. (c) Leininger, T.; Nicklass, A.; Stoll, H.; Dolg, M.; Schwerdtfeger, P. *J. Chem. Phys.* **1996**, *105*, 1052−1059.
(31) (a) McLean, A. D.; Chandler, G. S. *J. Chem. Phys.* **1980**, *72*, 5639−5648. (b) Krishnan, R.; Binkley, J. S.; Seeger, R.; Pople, J. A. *J. Chem. Phys.* **1980**, *72*, 650−654. (c) Wachters, A. J. H. *J. Chem. Phys.* **1970**, *52*, 1033−1036. (d) Hay, P. J. *J. Chem. Phys.* **1977**, *66*, 4377−4384. (e) Raghavachari, K.; Trucks, G. W. *J. Chem. Phys.* **1989**, *91*, 1062−1065. (f) Binning, R. C., Jr.; Curtiss, L. A. *J. Comput. Chem.* **1990**, *11*, 1206. (g) McGrath, M. P.; Radom, L. *J. Chem. Phys.* **1991**, *94*, 511−516.
(32) (a) Peng, C.; Ayala, P. Y.; Schlegel, H. B.; Frisch, M. J. *J. Comput. Chem.* **1996**, *17*, 49−56. (b) Peng, C.; Schlegel, H. B. *Isr. J. Chem.* **1993**, *33*, 449−454.
(33) (a) Carpenter, J. E.; Weinhold, F. *J. Mol. Struct. (Theochem)* **1988**, *169*, 41−62. (b) Carpenter, J. E. Ph.D. Thesis. University of Wisconsin, Madison, WI, 1987. (c) Foster, J. P.; Weinhold, F. *J. Am. Chem. Soc.* **1980**, *102*, 7211−7218. (d) Reed, A. E.; Weinhold, F. *J. Chem. Phys.* **1983**, *78*, 4066−4073. (e) Reed, A. E.; Weinhold, F. *J. Chem. Phys.* **1985**, *83*, 1736−1740. (f) Reed, A. E.; Weinstock, R. B.; Weinhold, F. *J. Chem. Phys.* **1985**, *83*, 735−746. (g) Reed, A. E.; Curtiss, L. A.; Weinhold, F. *Chem. Rev.* **1988**, *88*, 899−926. (h) Weinhold, F.; Carpenter, J. E. *The Structure of Small Molecules and Ions*; Plenum: New York, 1988; p 227.
(34) (a) McClean, A. D.; Chandler, G. S. *J. Chem. Phys.* **1980**, *72*, 5639−5648. (b) Krishnan, R.; Binkley, J. S.; Seeger, R.; Pople, J. A. *J. Chem. Phys.* **1980**, *72*, 650−654. (c) Wachters, A. J. H. *J. Chem. Phys.* **1970**, *52*, 1033−1036. (d) Hay, P. J. *J. Chem. Phys.* **1977**, *66*, 4377−4384. (e) Raghavachari, K.; Trucks, G. W. *J. Chem. Phys.* **1989**, *91*, 1062−1065. (f) Binning, R. C., Jr.; Curtiss, L. A. *J. Comput. Chem.* **1990**, *11*, 1206−1216. (g) McGrath, M. P.; Radom, L. *J. Chem. Phys.* **1991**, *94*, 511−516. (h) Clark, T.; Chandrasekhar, J.; Spitznagel, G. W.; Schleyer, P. v. R. *J. Comput. Chem.* **1983**, *4*, 294−301. (i) Frisch, M. J.; Pople, J. A.; Binkley, J. S. *J. Chem. Phys.* **1984**, *80*, 3265−3269.
(35) Zhao, Y.; Truhlar, D. G. *Theor. Chem. Acc.* **2008**, *120*, 215−241.
(36) (a) Zhao, Y.; Truhlar, D. G. *Acc. Chem. Res.* **2008**, *41*, 157−167. (b) Zhao, Y.; Truhlar, D. G. *Chem. Phys. Lett.* **2011**, *502*, 1−13.
(37) (a) Cancès, M. T.; Mennucci, B.; Tomasi, J. *J. Chem. Phys.* **1997**, *107*, 3032−3041. (b) Cossi, M.; Barone, V.; Mennucci, B.; Tomasi, J. *Chem. Phys. Lett.* **1998**, *286*, 253−260. (c) Mennucci, B.; Tomasi, J. *J. Chem. Phys.* **1997**, *106*, 5151−5158. (d) Tomasi, J.; Mennucci, B.; Cammi, R. *Chem. Rev.* **2005**, *105*, 2999−3094.
(38) Marenich, A. V.; Cramer, C. J.; Truhlar, D. G. *J. Phys. Chem. B* **2009**, *113*, 6378−6396.